ESTIMATES OF FOREST GROWING STOCK VOLUME OF THE NORTHERN HEMISPHERE FROM ENVISAT ASAR

Maurizio Santoro [(1)], Christiane Schmullius [(2)], Carsten Pathe [(2)], Julian Schwilk [(2)], Christian Beer [(3)], Martin Thurner [(4)], Johan E. S. Fransson [(5)], Anatoly Shvidenko [(6)], Dmitry Schepaschenko [(6)], Ian McCallum [(6)], Ronald J. Hall [(7)], André Beaudoin [(8)]

[(1)] Gamma Remote Sensing, Worbstrasse 225, 3073 Gümligen, Switzerland, Email: santoro@gamma-rs.ch
[(2)] Department of Earth Observation, Friedrich-Schiller University, 07743 Jena, Germany; Email: c.schmullius@uni-jena.de, carsten.pathe@uni-jena.de, julian.schwilk@uni-jena.de
[(3)] Department of Applied Environmental Science (ITM) and Bert Bolin Centre for Climate Research, Stockholm University, Sweden; Email: christian.beer@itm.su.se
[(4)] Max Planck Institute for Biogeochemistry, Jena, Germany, E-Mail: mthurn@bgc-jena.mpg.de
[(5)] Department of Forest Resource Management, Swedish University of Agricultural Sciences, 901 83 Umeå, Sweden, Email: johan.fransson@slu.se
[(6)] International Institute of Applied Systems Analysis, 2361 Laxenburg, Austria, Email: shvidenk@iiasa.ac.at, schepd@iiasa.ac.at, mccallum@iiasa.ac.at
[(7)] Natural Resources Canada, Canadian Forest Service, Northern Forestry Centre, Edmonton, Alberta, Canada T6H 3S5, Email: Ron.Hall@NRCan-RNCan.gc.ca
[(8)] Natural Resources Canada, Canadian Forest Service, Laurentian Forestry Centre, Sainte-Foy, Québec, Canada G1V 4C7, Email: Andre.Beaudoin@RNCan-NRCan.gc.ca

ABSTRACT

This paper presents and assesses a dataset of forest growing stock volume (GSV) above 30°N estimated from multi-temporal backscatter measurements acquired by Envisat Advanced Synthetic Aperture Radar (ASAR) in ScanSAR mode. The retrieval was based on the BIOMASAR algorithm that combines standard SAR processing techniques for multi-temporal SAR data and an automated GSV estimation approach based on a Water Cloud-like model and a weighted combination of GSV estimates from individual measurements of the SAR backscatter. Approximately 70,000 ASAR images were used to estimate GSV at a pixel size of 0.01°. Assessment of the retrieved GSV indicated (i) the importance of comparing to reference data at the same scale, (ii) moderate agreement with reference datasets at full resolution because of the limited sensitivity of C-band SAR backscatter to GSV, (iii) strong agreement with reference datasets after aggregation at regional and national level, (iv) consistent retrieval results throughout the study area, (v) saturation at approximately 300 m^3/ha.

1. INTRODUCTION

The feasibility of mapping forest variables, such as canopy height or above-ground biomass, at continental and global scale with spaceborne remote sensing data has increased in recent years because of the availability of datasets with full and repeated coverage within short periods of time [1]. Synthetic Aperture Radar (SAR) intensity is particularly suitable for retrieval of the forest growing stock volume (GSV), i.e., the density of tree trunks per unit area, because forest structural properties affect the signal backscattered from a forest. The availability of large stacks of backscatter measurements acquired by Envisat ASAR in ScanSAR mode has favoured the development of an approach, referred to as BIOMASAR, to retrieve forest growing stock volume (GSV) from hyper-temporal datasets of C-band backscatter [2]. With respect to a retrieval based on single images, a hyper-temporal approach increases the accuracy because images with stronger sensitivity of the backscatter are given more weight. An assessment of the capability of the BIOMASAR retrieval algorithm to generate large-scale estimates of GSV in three regions within the boreal zone indicated consistent estimates and correct representation of the spatial distribution of GSV [3]. The weak sensitivity of C-band backscatter to forest structural parameters introduced significant uncertainty to the estimated GSV at full resolution (0.01°, corresponding to 1 km). Aggregated estimates to 0.1° and 0.5° were characterized by stronger agreement with respect to reference datasets of GSV. The relative difference at 0.5° was consistently within a magnitude of 20-30% [3].

This paper presents a dataset of forest GSV representative of the year 2010 estimated from Envisat ASAR ScanSAR data. The study area covered the North American and Eurasian continent, roughly corresponding to land masses above 30°N latitude. The area included the boreal and hemi-boreal forest zones, as well as temperate forests to a large extent. The estimates of GSV were validated with *in situ* measurements, where available, or verified with respect

to other estimates of GSV, typically obtained from other Earth Observation (EO) datasets. The GSV dataset can be downloaded from a dedicated BIOMASAR website (http://www.biomasar.org). It can also be viewed and validated on the Biomass Geo-Wiki website (http://biomass.geo-wiki.org)

2. BIOMASAR ALGORITHM

The BIOMASAR algorithm consists of a SAR processing block that generates stacks of co-registered images of the SAR backscatter and a GSV retrieval block whereby the SAR backscatter observations are input to a model of the forest backscatter to obtain single estimates of GSV. These estimates are subsequently weighted to obtain the final estimate of GSV. The retrieval algorithm has been described in [2] whereas the implementation to derive the estimates of GSV has been described in [3].

SAR processing consisted of standard approaches to generate a co-registered, calibrated, speckle reduced and topography-normalized dataset of SAR backscatter measurements (see also Section 3). GSV was retrieved by training a Water Cloud-like model and inverting this for each observation. This step was implemented on a pixel-by-pixel basis and run automatically without the need of training data for the forest backscatter model. The two unknown model parameters were estimated from central tendency statistics of the backscatter for unvegetated areas and areas with high canopy cover within estimation windows centred at the pixel of interest. Percentage of canopy cover was derived from the MODIS Vegetation Continuous Fields (VCF) product [4].

The model training and the retrieval required an estimate of GSV for dense forest and maximum retrievable GSV, i.e., an average GSV of the densest forest and the largest realistic GSV value typical of the area where the pixel of interest is located. In [2], it was reported that the two parameters present a relatively constant difference of 50 m^3/ha. Hence, setting the former also allows defining the range of retrievable GSVs. Where continuous fields of GSV were available in form of a raster dataset, the GSV of dense forest corresponds to the 90th percentile of the histogram [2]. The value was set empirically when only statistics from inventory reports were available. It is assumed that a single value of GSV of dense forest is representative for a 2° × 2° area. To obtain a smooth transition of the GSV of dense forest between adjacent tiles, the individual values were interpolated using a bilinear function. An offset in the estimate of GSV of dense forest translated to a systematic bias of the retrieval [2]. If the retrieved GSV aggregated at very coarse scale (e.g. 2° or more) appeared systematically biased over a large area spanning several tiles with respect to a reference dataset of GSV, the GSV of dense forest had to be fine tuned until the bias was minimized.

Assuming N observations of the SAR backscatter, N estimates of GSV were obtained by inverting the corresponding trained model. The N GSV estimates were linearly weighted to form the final GSV estimate. The weights were set equal to the image-specific difference between the modelled backscatter for the densest forest and an unvegetated area, normalized with the maximum difference. Observations characterized by a backscatter contrast below 0.5 dB were discarded because they would not contribute to the GSV estimate.

3. SAR DATASET

To obtain estimates of GSV representative for the year 2010, we used Envisat ASAR ScanSAR data acquired between October 2009 and February 2011. The time span included two winter seasons in order to maximize the number of winter/frozen datasets. The frozen conditions were shown to be most suitable for the retrieval in the boreal zone [6]. To further maximize the vector of SAR backscatter observations, images acquired in both Wide Swath Mode (75 m pixel size) and Global Monitoring Mode (500 m pixel size) were selected. Gap fillers with data acquired afterwards until the end of the Envisat mission (April 2012) were necessary for Japan, southwest United States, southwest Alaska and St. Pierre and Miquelon (Canada). Approximately 70,000 image strips were selected for processing. Fig. 1 shows the number of backscatter observations per pixel after processing. Wall-to-wall coverage was obtained for North America, Korea and Japan above 30°N and for Eurasia above 34°N. Central and east Greenland and islands of the northern hemisphere were not considered because unvegetated.

SAR data processing was undertaken on the European Space Agency (ESA) Grid Processing on Demand (G-POD) environment (http://gpod.eo.esa.int/). To optimize computing resources on the G-POD platform, the study area had to be divided into 23 processing sub-regions with further temporal sub-setting [5]. Each SAR image was multi-looked to 1 km and then terrain geocoded to equiangular projection and a pixel spacing of 0.01°. Screening of the geocoded SAR data showed high radiometric consistency and geometric accuracy at the sub-pixel level. The individual images were tiled according to a 2° × 2° grid for flexible management of the large dataset. Speckle was reduced with a multi-temporal filter [6] with weights starting from a speckle-reduced dataset obtained with the GAMMA MAP filter. Radiometric normalization for slope-induced effects on the SAR backscatter was applied in the output geometry using an estimate of pixel area and local incidence angle [7].

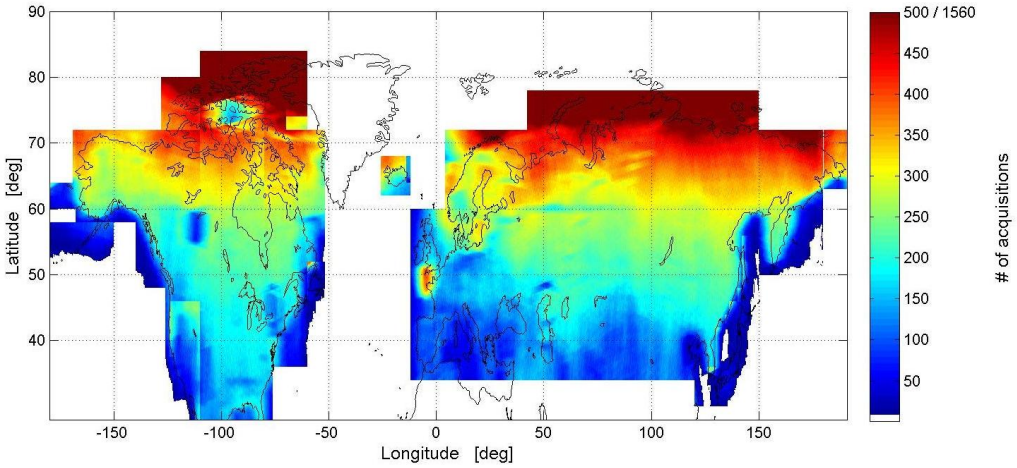

Figure 1. Number of SAR backscatter observations per pixel for the Envisat ASAR ScanSAR dataset used to retrieve forest GSV. The colour bar has been constrained between 0 and 500 observations to enhance the image contrast.

Terrain geocoding and normalization of backscatter for slope-induced effects was supported by an in-house built global Digital Elevation Model (DEM). The SRTM DEM [8] (version 4.1) was completed with digitized topographic maps [9] for the northern latitudes of Eurasia, the Canadian Digital Elevation Database [10] and the USGS 7.5 minutes native DEM over Alaska [11] to form a seamless global dataset of elevation. The global dataset was obtained at 3 arc-seconds; a 0.01° version was obtained by boxcar averaging (12 × 12 window) and resampling with a bilinear interpolation.

4. GSV ESTIMATES

The SAR dataset was used to generate the map of forest GSV representative for the year 2010 (Fig. 2). A first map was generated on G-POD; fine tuning of the GSV of dense forest was required locally and was completed on local servers. GSV estimates were obtained for all land pixels except those belonging to urban or water or snow/ice land-cover classes. The backscatter from such areas strongly impacts the model training by causing an offset of the model parameters; hence, they need to be masked out *a priori*. The urban mask was based on the MODIS map of global urban extent [12]. The water mask was based on the water class in the GlobCover 2005 land cover dataset [13] below 60°N and the GLC2000 land cover dataset [14] elsewhere. Snow/ice pixels were identified by means of the GLC2000 map. Classification errors in these datasets resulted in an error in the GSV map in the sense that GSV was not mapped in the case of a commission error whereas it was incorrectly estimated in the case of an omission error.

Local voids in forest land corresponded mostly to areas where the GSV estimate was based upon less than ten SAR observations retained for the multi-temporal GSV combination (Table 1). Non-forest land (cropland, shrubland and grassland) was characterized by more frequent and larger voids; nonetheless, such voids are of minor importance since the estimated GSV is likely to be unrealistic considering that the backscatter model used to link the SAR backscatter to the GSV is parameterized to represent the scattering occurring in a forest.

The GSV estimates in Fig. 2 agree with the real patterns of the GSV distribution in the boreal and temperate zones. The highest GSV occurred along the Pacific Northwest Coast in North America, Central Europe, Central Siberia, the Russian Far East along the Pacific coast and Japan. Latitudinal and longitudinal gradients of GSV related to regional climatic conditions were well reproduced.

The number of SAR observations retained for the multi-temporal combination is shown in Fig. 3. With respect to the total number of observations, this dataset indicates how many observations were used to form the multi-temporal estimate of GSV. The difference between datasets in Fig. 1 and Fig. 3 is clear over North America between 50°N and 60°N; while the number of observations available was rather homogeneous (approximately 250) almost everywhere within this belt, the number of observations retained for the multi-temporal retrieval was different depending on several factors (local environmental conditions, topography etc.). The dataset in Fig. 3 represents a quality flag for the estimated GSV; the higher the number of observations, the more reliable the estimate of GSV. Areas with less than 10 backscatter observations retained for the retrieval were masked out because they were likely to be erroneous. A layer of pixel-based uncertainties is currently being derived.

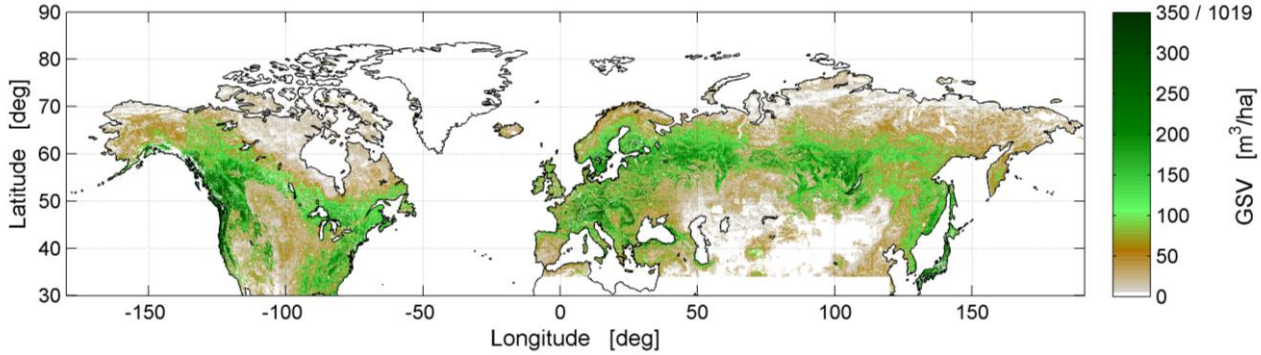

Figure 2. GSV estimated from Envisat ASAR data. The colour bar is constrained between 0.1 and 350 m^3/ha, while the retrieved GSV reached up to 1,019 m^3/ha. The percentage of pixels with GSV > 350 m^3/ha was 0.3%. Zero was assigned to unmapped pixels and pixels for which the number of SAR observations used for retrieval was less than 10 (i.e., unreliable estimates).

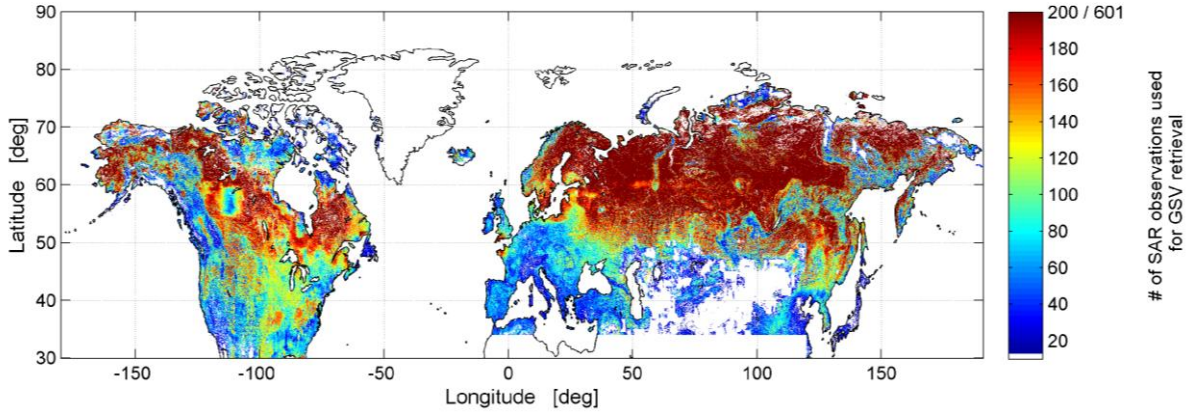

Figure 3. Number of SAR observations used for the GSV retrieval shown in Fig. 2. The colour bar is constrained between 10 and 200, while the number of observations used reached up to 601. As in Fig. 2, zero was assigned to unmapped pixels and pixels for which the number of SAR observations used for retrieval was less than 10 (i.e., unreliable estimates).

Table 1. Explanation and location of voids in SAR-based GSV data product (only forest land considered).

Explanation	Location
Too few SAR measurements	• Southwest Alaska, • Southwest US, • Italy, • Japan, • Inner Mongolia, • Verkhoyansk and East Siberian range
Incorrect urban mask	• Occasionally in the US Mid-west
Insufficient number of pixels to estimate the model parameters	• Islands along east coast of North America, • Coastline of north Spain
Mixed cropland/forest landscape	• Turkey, • Kazakhstan

5. VERIFICATION OF GSV ESTIMATES

The verification of the GSV estimates was carried out at the native resolution (0.01°) as well as at the aggregated level by comparing against *in situ* as well as EO-based estimates of GSV. Several aggregation levels were considered, ranging from typical pixel sizes used by carbon models (0.1° and 0.5°) to regional and national scale. The agreement between the ASAR GSV estimates and GSV measurements in ancillary datasets to be used as reference has been quantified by means of the Pearson's correlation coefficient (r) and the Root of the Mean Squared Deviation (RMSD) relative to the mean value of GSV of the reference dataset. Statistics are reported for forest area, which was identified by means of a combination of the GLC2000 and GlobCover 2005 land cover products. Herewith, we tried to avoid that product-specific flaws could affect the results. Primarily in areas of fragmented forest landscapes, the impact of the land cover dataset used as forest mask on the averaged GSVs was not negligible (see also [3])

The drawback of using *in situ* measurements is the much finer scale at which GSV is typically represented compared to the 1 km scale of the ASAR dataset. In addition, their distribution is often too coarse to allow a reliable extrapolation to obtain a two-dimensional representation of GSV comparable to the spatial distribution in the ASAR dataset. Fig. 4 shows a comparison between retrieved GSV and GSV based on plot-wise measurements of the Swedish National Forest Inventory (NFI). A single forest inventory plot covers an area with a radius of 7 or 10 m; within a 1 km^2 area there are at most 10-15 plots. The NFI samples only a minor fraction of the area covered by a single ASAR pixel. The different scales at which GSV is described in the two datasets explain the large scatter and the very limited agreement between NFI and ASAR estimates of GSV at 0.01° (Fig. 4, top). Aggregation to a very coarse spatial resolution such as 0.5° implies that several plot-based GSV estimates are averaged together to form a new estimate where the scale is more in line with the scale of the ASAR dataset. Aggregation cells with the largest number of NFI plots present stronger agreement with the corresponding GSV estimate from the ASAR data (Fig. 4, bottom).

A comparison against EO-based raster datasets of GSV is less affected by scale issues [3], thus allowing to benchmark the level of information as well as errors in the ASAR dataset in a more reliable manner. Fig. 5 shows the agreement between ASAR GSV and a reference GSV dataset based on EO data and local *in situ* measurements [15] for Russia at the full 0.01° resolution and at the 0.5° aggregated level. At full resolution, the agreement between the datasets was moderate (Fig. 5, left; r = 0.55, Rel. RMSD = 62.9%). The red line corresponding to the regression between the two datasets indicates higher estimates by ASAR in low GSV forest and smaller estimates by ASAR in high GSV forest. This result was interpreted as a consequence of inconsistencies and limitations of each dataset since both rely on datasets that are only partially related to GSV. The overestimation over areas of low biomass and underestimation over areas of high biomass was consistent with other studies that have employed remote sensing and inventory data at several scales using a variety of methods and data sources [16, 17].

For increasing aggregation, the agreement between the datasets increased. At 0.5°, the agreement was strong (Fig. 5, right; r = 0.89, Rel. RMSD = 30.7%). The regression line highlights slightly less GSV in the ASAR dataset for the highest GSV. The few outliers were identified in a difference map between the ASAR and the reference dataset and revealed that the ASAR dataset presented flaws in correspondence of steep topography, land fragmentation and underestimated range of retrievable GSV. While the latter can be corrected for by fine tuning the retrieval, the other issues are inherent to the SAR system

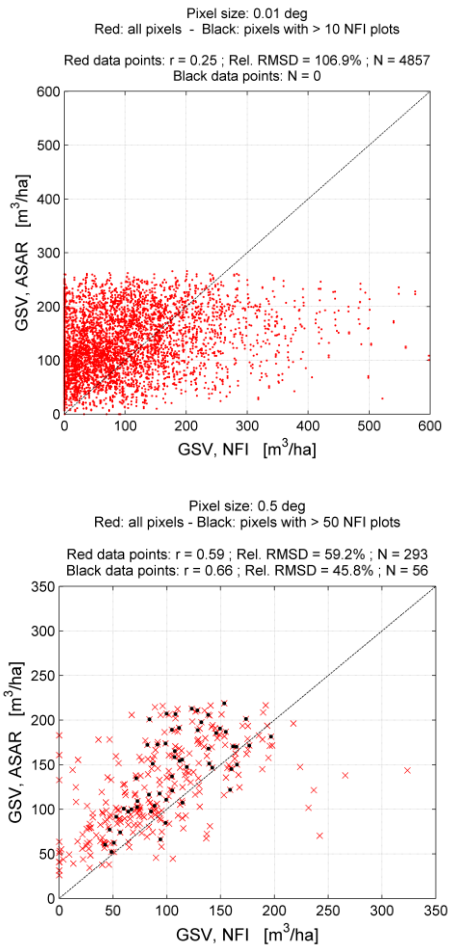

Figure 4. Scatterplot of ASAR GSV and GSV derived from NFI for Sweden at 0.01° (top) and 0.5° (bottom) pixel size.

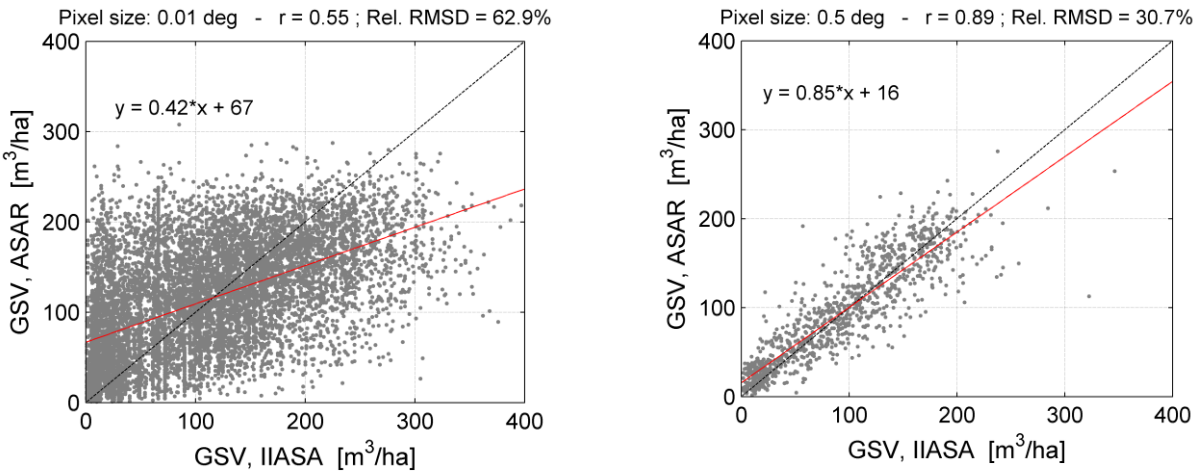

Figure 5. Scatterplot of ASAR GSV and GSV derived from inventory data scaled by EO (IIASA GSV) [15] for Russia at 0.01° (left) and 0.5° (right) pixel size. The red line represents the regression to the two datasets.

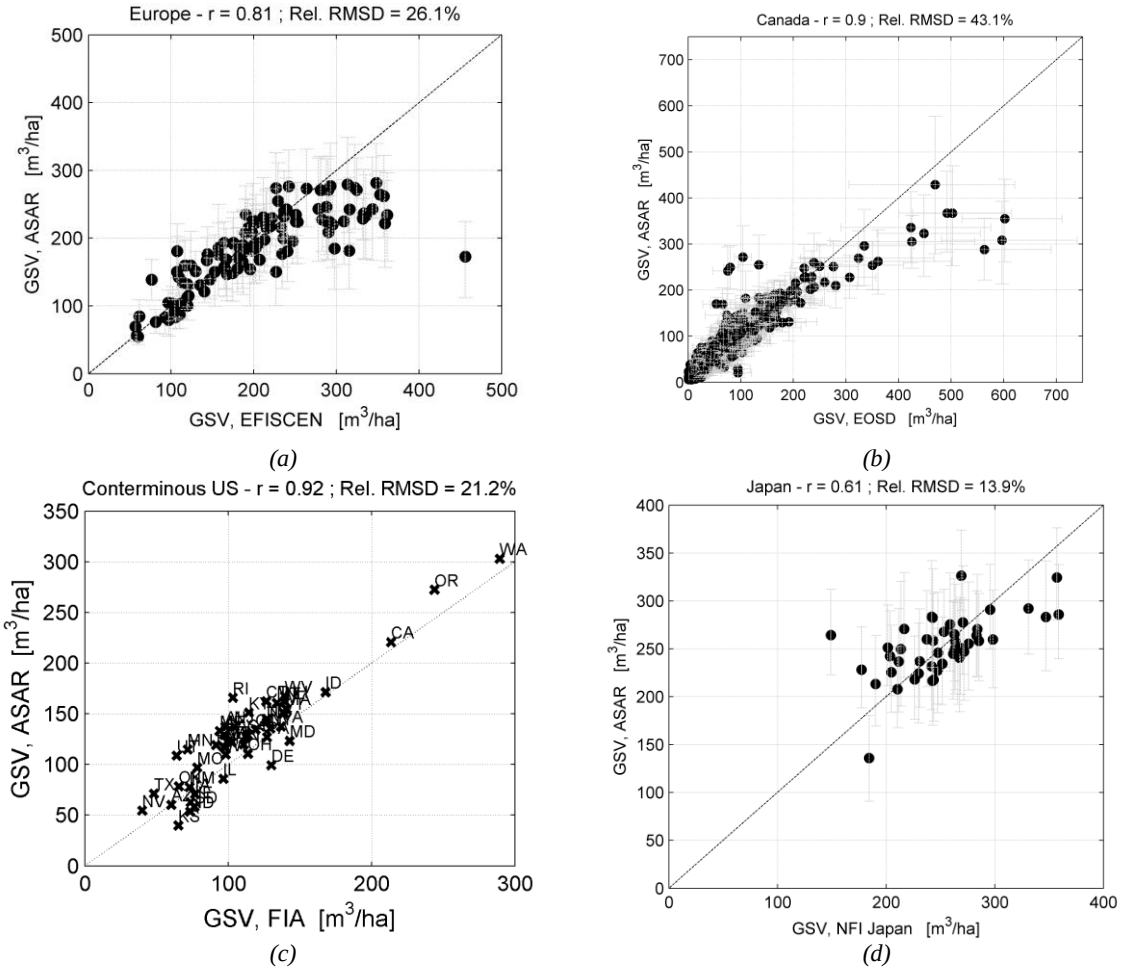

Figure 6. Scatterplot of ASAR GSV (y-axis) with respect to GSV from (a) European Forest Institute Database EFISCEN at provincial/national level [18], (b) EOSD estimates of total volume aggregated to 2° [19], (c) US Forest Inventory and Analysis database [20] aggregated at state level for the conterminous states, (d) Japanese NFI at prefecture level (courtesy F. Kitahara, http://www.rinya.maff.go.jp/).

The consistency of the GSV retrieval throughout the study area is illustrated in Fig. 6 where aggregated estimates of GSV from the ASAR dataset are compared to corresponding estimates derived from national inventory or EO datasets of GSV. Despite different origins, inventory and retrieval methods, timing of the datasets, the agreement between ASAR and reference datasets was strong up to until approximately 300 m^3/ha. Above this level, the ASAR GSV started saturating in Canada and Europe whereas for the conterminous US and Japan the trend was not as clear. The trend of underestimation could be explained as a consequence of the lack of sensitivity of the C-band SAR backscatter to GSV for very high GSVs. For large proportion of very high GSV and high overall GSV within the aggregation unit, we observed the largest discrepancy between the ASAR GSV and the reference GSV. Most underestimation took place in central Europe, between Luxembourg and Czech Republic, and along the Pacific Northwest coast. In addition, very patchy landscapes of small forests with high GSV within pasture and agricultural land caused further substantial underestimation in the ASAR GSV dataset because this does not separate between land cover at sub-pixel level.

6. DISCUSSION AND CONCLUSIONS

This paper presented estimates of forest GSV representative of the year 2010 for latitudes north of 30°N derived from multi-temporal C-band Envisat ASAR ScanSAR images of the radar backscatter. This study represents an unprecedented attempt to generate estimates of GSV across the boreal and temperate zones with a single retrieval approach. While some aspects of the retrieved GSV have been clearly assessed, others require further investigation.

The assessment of the retrieved GSV at the full resolution (0.01°) and at the aggregated level indicated:

1. Consistent estimates of GSV across three continents:
    a. agreement with reference datasets up to approximately 300 m^3/ha,
    b. underestimation for GSV > 300 m^3/ha
    c. large scatter with respect to the reference dataset at full resolution (0.01°),
    d. increased agreement for increasing aggregation level,
    e. relative difference with respect to reference data on the order of 15-30% at aggregated level (> 0.5°).
2. Agreement of the spatial distribution of the GSV with respect to existing datasets at similar spatial resolution.

The assessment also indicated a number of shortcomings and bottlenecks when dealing with coarse resolution data in an environment of limited data availability to be used as reference. Forest plot inventory data are not suitable for validation because the measurement at the scale of a plot represents a different forest structure and composition compared to the kilometric scale of the ASAR data. The relative difference on the order of 60-100% obtained in Sweden and Siberia do not represent true retrieval statistics. Inventory units at 1 km scale suitable for correct validation of GSV estimates derived from low resolution remote sensing data are highly desirable but practically do not exist in such form. Hence, rigorous validation of such GSV estimates is not possible. Inventory data aggregated at lower spatial resolution present less spatial heterogeneity, thus containing information that is closer to the estimate obtained from remote sensing at coarse resolution. The drawback of comparing aggregated measurements of GSV from inventory data and remote sensing based estimates of GSV is the impossibility to provide conclusions on the spatial distribution of the estimated GSV. Dealing with a research area that included several countries, requires a thorough screening and interpretation of the data to be used as reference. Typically, large-scale averages at the level of provinces, counties or countries are sufficiently reliable to act as reference over large areas.

Future investigation shall focus on understanding of the GSV estimates systematic flaws. According to a first screening of these, the influence on the retrieved GSV of sloped terrain, land cover type and land cover fragmentation, and snags/dead wood need to be assessed in a more quantitative way. Also of interest is a comparison of scales, i.e. among retrieved GSV from different ASAR modes between 20 m and 1 km. This latter aspect is of particular interest with the availability of data from the forthcoming Sentinel-1 mission.

7. ACKNOWLEDGMENTS

This study was supported by the European Space Agency (ESA) within the Support to Science Element (STSE) project BIOMASAR (ESRIN contract No. 21892/08/I-EC). M. Engdahl and D. Fernandez Prieto, ESA, are acknowledged for support and scientific advice. R. Cuccu, S. Pinto and J. Farres are greatly acknowledged for implementation of the processing chain on G-POD and technical support. Envisat ASAR data have been distributed under ESA's Category-1 project nr. 6397. Access to G-POD was obtained under ESA's Category-1 project nr. 9209.

8. REFERENCES

1. Schepaschenko, D., See, L., Fritz, S., McCallum, I., Schill, C., Perger, C., Baccini, A., Gallaun, H., Kindermann, G., Kraxner, F., Saatchi, S.,

Obersteiner, M., Santoro, M., Schmullius, C., Shvidenko, A. & Schepaschenko, M. (2012). Observing forest biomass globally. *Earthzine*.

2. Santoro, M., Beer, C., Cartus, O., Schmullius, C., Shvidenko, A., McCallum, I., Wegmüller, U. & Wiesmann, A. (2011). Retrieval of growing stock volume in boreal forest using hyper-temporal series of Envisat ASAR ScanSAR backscatter measurements. *Remote Sens. Environ.* **115**(2), 490-507.
3. Santoro, M., Cartus, O., Fransson, J.E.S., Shvidenko, A., McCallum, I., Hall, R.J., Beaudoin, A., Beer, C. & Schmullius, C. (in press). Estimates of forest growing stock volume for Sweden, Central Siberia and Québec using Envisat Advanced Synthetic Aperture Radar backscatter data. *Remote Sensing*.
4. Hansen, M.C., De Fries, R.S., Townshend, J.R.G., Carroll, M., Dimiceli, C. & Sohlberg, R.A. (2003). Global percent tree cover at a spatial resolution of 500 meters: First results of the MODIS Vegetation Continuous Field algorithm. *Earth Interact.* **7**(10), 1-15.
5. Santoro, M., Schmullius, C., Pathe, C. & Schwilk, J. (2012). Pan-boreal mapping of forest growing stock volume using hyper-temporal Envisat ASAR ScanSAR backscatter data. In Proc. IGARSS'12, IEEE Publications, Piscataway, NJ, pp 7204-7207.
6. Quegan, S. & Yu, J.J. (2001). Filtering of multichannel SAR images. *IEEE Trans. Geosci. Remote Sensing* **39**(11), 2373-2379.
7. Wiesmann, A., Wegmüller, U., Santoro, M., Strozzi, T. & Werner, C. (2004). Multi-temporal and multi-incidence angle ASAR Wide Swath data for land cover information. In Proc. 4th International Symposium on Retrieval of Bio- and Geophysical Parameters from SAR Data for Land Applications, CD-ROM.
8. Rabus, B., Eineder, M., Roth, A. & Bamler, R. (2003). The Shuttle Radar Topography Mission - A new class of digital elevation models acquired by spaceborne SAR. *ISPRS Journal of Photogrammetry & Remote Sensing* **57**, 241-262.
9. de Ferranti, J. (2009). Digital Elevation Data. http://www.viewfinderpanoramas.org/dem3.html. Accessed on 28 February 2012.
10. Anon. (2007). Canadian Digital Elevation Data. http://www.geobase.ca/geobase/en/index.html. Accessed on 28 February 2012.
11. Anon. 7.5-Min DEM Native Format of the United States. http://www.webgis.com/. Accessed on 28 February 2012.
12. Schneider, A., Friedl, M.A. & Potere, D. (2009). A new map of global urban extent from MODIS satellite data. *Environ. Res. Lett.* **4**, 044003.
13. Bicheron, P., Defourny, P., Brockmann, C., Schouten, L., Vancutsem, C., Huc, M., Bontemps, S., Leroy, M., Achard, F., Herold, M., Ranera, F. & Arino, O. (2008). GLOBCOVER – Products Description and Validation Report. Media France.
14. Bartholomé, E. & Belward, A.S. (2005). GLC2000: A new approach to global land cover mapping from Earth Observation data. *Int. J. Remote Sens.* **26**(9), 1959-1977.
15. Schepaschenko, D., Mc Callum, I., Shvidenko, A., Fritz, S., Kraxner, F. & Obersteiner, M. (2011). A new hybrid land cover dataset for Russia: A methodology for integrating statistics, remote sensing and in situ information. *Journal of Land Use Science* **6**(4), 245-259.
16. Hall, R.J., Skakun, R.S. & Arsenault, E.J. (2006). Modeling forest stand structure attributes using Landsat ETM+ data: application to mapping of aboveground biomass and stand volume. *For. Ecol. Manage.* **225**, 378-390.
17. Gallaun, H., Zanchi, G., Nabuurs, G.J., Hengeveld, G., Schardt, M. & Verkerk, P.J. (2010). EU-wide maps of growing stock and above-ground biomass in forests based on remote sensing and field measurements. *For. Ecol. Manage.* **260**(3), 252-261.
18. Schelhaas, M.J., Varis, S., Schuck, A. & Nabuurs, G.J. (2006). EFISCEN Inventory Database. http://www.efi.int/portal/virtual_library/databases/efiscen/. Accessed on 7 January 2013.
19. Hall, R.J., Skakun, R.S., Beaudoin, A., Wulder, M.A., Arsenault, E.J., Bernier, P.Y., Guindon, L., Luther, J.E. & Gillis, M.D. (2010). Approaches for forest biomass estimation and mapping in Canada. In Proc. IGARSS'10, IEEE Publications, Piscataway, NJ, pp 1988-1991.
20. O'Connell, B.M., LaPoint, E.B., Turner, J.A., Ridley, T., Boyer, D., Wilson, A.M., Waddell, m.K.L. & Conkling, B.L. (2012). FIA Database Description and Users Manual for Phase 2. USDA Forest Service, Arlington, VA version 5.1.2, http://www.fia.fs.fed.us/library/database-documentation/.